

# $B$ decays into light scalar particles and glueball<sup>\*</sup>

P. Minkowski<sup>1,a</sup>, W. Ochs<sup>2,b</sup>

<sup>1</sup> University of Bern, 3012 Bern, Switzerland

<sup>2</sup> Max-Planck-Institut für Physik, Werner-Heisenberg-Institut, 80805 Munich, Germany

Received: / 23 April 2004 / Revised version: 27 October 2004 /

Published online: 21 December 2004 – © Springer-Verlag / Società Italiana di Fisica 2004

**Abstract.** The recent observations of  $f_0(980)$  in charmless  $B$  decays motivate further studies of scalar particle and glueball production in these processes. Amplitudes for charmless two-body  $B$  decays involving the members of the scalar nonet are presented based on the symmetries of the dominant penguin contribution. Different scenarios for the lightest scalar nonet are investigated in view of the presently available data. We describe the evidence from  $B$  decays for  $f_0(1500)$  with a flavor octet like mixing and the hints towards the members of the  $q\bar{q}$  nonet of lowest mass. There is further support for the hypothesis of a broad  $0^{++}$  glueball acting as coherent background especially in  $B \rightarrow K\bar{K}K$ . The estimated  $B$  decay rates into gluonic mesons represent a sizable fraction of the theoretically derived decay rate for  $b \rightarrow sg$ .

## 1 Introduction

A longstanding problem in QCD is the prediction of gluonic boundstates (“glueballs”) and the lack of certainty in their identification. The lightest glueball is expected in the scalar channel with  $J^{PC} = 0^{++}$ . In this channel there is a series of established resonances but also various broad objects whose existence is not generally accepted. There is also no consensus about the lightest scalar  $q\bar{q}$  nonet, neither about its members nor about the mixing between strange and non-strange components. A central issue is the nature of  $f_0(980)$  which has been considered not only as standard  $q\bar{q}$  meson but also as a  $K\bar{K}$  molecule or as  $qq\bar{q}\bar{q}$  state.

There are now new experimental results on charmless  $B$  decays into scalar particles which provide additional information of high statistics. In this paper we discuss some recent results and their implications on scalar spectroscopy. (1) The observation by the BELLE [1–4] and BaBar Collaborations [5, 6] of charmless decays  $B \rightarrow Kh^+h^-$  with  $h = \pi, K$  with a significant peak related to  $f_0(980)$  and some less pronounced signals from other scalars.

(2) In the channel  $B \rightarrow K\bar{K}K$  BELLE has also observed a broad enhancement (coherent “background”) in the  $K\bar{K}$  mass spectrum in the range 1000–1700 MeV and perhaps beyond with spin  $J = 0$  and a smaller effect in  $\pi\pi$  around 1000 MeV. Similar results are shown by BaBar but there is no quantitative analysis yet.

Remarkably, in  $B$  decays, as compared to decays of charmed  $D$  or  $J/\psi$  mesons the role of scalar particles is more pronounced because of the larger phase space and

therefore reduced background from crossed channels and also because of an apparent suppression of higher spin ( $J = 2$ ) states. In this paper we will discuss what can be concluded from the above observations and how further experimental studies can uncover the members of the light scalar nonet besides  $f_0(980)$  and possibly help to identify the gluonic interaction related to the  $0^{++}$  glueball. Some considerations concerning earlier data have been presented already in [7]. Other pertinent results concern the observation of  $f_0(980)$  and gluonic mesons in gluon jets [7, 8]. Not much theoretical work so far has been concerned with  $B$  decays into scalar particles. Some selected  $B$  decays into flavored scalar mesons have been derived from a factorization ansatz for the effective weak Hamiltonian including power corrections  $\mathcal{O}(\Lambda/m_b)$  [9].

The interest in charmless  $B$  decays with strangeness has been stimulated through the observation by CLEO [10, 11] of large inclusive and exclusive decay rates  $B \rightarrow \eta'X$  and  $B \rightarrow \eta'K$ , which have been confirmed by more recent measurements [12–14]. These processes have been related to the decay  $b \rightarrow sg$  of the  $b$ -quark which could be a source of mesons with large gluon affinity [15–18]. In consequence, besides  $\eta'$ , also other gluonic states, in particular also scalar mesons or glueballs, could be produced in a similar way.

The total rate  $b \rightarrow sg$  has been calculated perturbatively in leading [19] and next-to-leading order [20]:

$$\begin{aligned} \mathcal{B}(b \rightarrow sg) & \quad (1) \\ & = \begin{cases} (2-5) \times 10^{-3} & \text{in LO (for } \mu = m_b \dots m_b/2), \\ (5 \pm 1) \times 10^{-3} & \text{in NLO.} \end{cases} \end{aligned}$$

The energetic massless gluon in this process could turn entirely into gluonic mesons by a non-perturbative transition after color neutralization by a second gluon. Alternatively,

<sup>\*</sup> Work supported in part by the Schweizerischer Nationalfonds.

<sup>a</sup> e-mail: mink@itp.unibe.ch

<sup>b</sup> e-mail: wwo@mppmu.mpg.de

color neutralization through  $q\bar{q}$  pairs is possible as well. This is to be distinguished from the short distance process  $b \rightarrow s\bar{q}q$  with virtual intermediate gluon which has to be added to the CKM-suppressed decays  $b \rightarrow q_1\bar{q}_2q_2$ . These quark processes with  $s$  have been calculated and amount to branching fractions of  $\sim 2 \times 10^{-3}$  each [20–22]. The question then arises which hadronic final states correspond to the decay  $b \rightarrow sg$ .

We recall that a large gluonic penguin component has been suggested to play also an important if not dominant role in the explanation of the  $\Delta I = \frac{1}{2}$  rule in  $K$  decay [23].

Next we outline the status of the phenomenological discussion concerning the light scalar spectroscopy. The Particle Data Group [24] lists below 1800 MeV the following isoscalar particles:

$$f_0(600) \text{ (or } \sigma), f_0(980), f_0(1370), \\ f_0(1500), f_0(1710); \quad (2)$$

furthermore the isovectors  $a_0(980)$ ,  $a_0(1450)$  and the strange  $K_0^*(1430)$ , and possibly there are  $\kappa(850)$  and  $K_0^*(1950)$ . The broad states  $\sigma, \kappa$  are still controversial, and also not much reliable information is available about  $f_0(1370)$ . The states listed above should be related to a scalar  $q\bar{q}$  nonet and, possibly, a glueball.

Quantitative results on glueballs are derived today from the QCD lattice calculations or QCD sum rules. Both agree that the lightest glueball has quantum numbers  $J^{PC} = 0^{++}$ .

Lattice calculations in quenched approximation [25–28] (without light sea quark–antiquark pairs) suggest the lightest glueball to have a mass in the range 1400–1800 MeV [29]. Results from unquenched calculations still suffer from systematic effects, the large quark masses of the order of the strange quark mass and large lattice spacings. Typically, present results on the glueball mass are about 20% lower than the quenched results [30, 31].

Results on glueballs have also been obtained from QCD sum rules. Recent calculations [39] for the  $0^{++}$  glueball yield a mass consistent with the quenched lattice result but in addition require a gluonic state near 1000 MeV. Similar results with a low glueball mass around 1000 MeV are obtained also in other calculations [40]. On the other hand, it has been argued [41] that the sum rules can also be saturated by a single glueball state with mass 1250  $\pm$  200 MeV.

In conclusion, there is agreement in the QCD based calculations on the existence of a  $0^{++}$  glueball, but the mass and width of the lightest state are not yet certain and phenomenological searches should allow for a mass range of about 1000–1800 MeV.

In the interpretation of the phenomenological results one can identify two major different directions of thought; they differ in the role of  $f_0(980)$  which belongs either to a nonet with particles of higher mass or with particles of lower mass.

#### Route A: Scalar nonet with $f_0(980)$ and heavier particles

In a previous study [32] we have performed a detailed phenomenological analysis of the production and decay of

low mass scalar mesons, which led us to identify the lightest  $q\bar{q}$  scalar nonet with the states

$$f_0(980), a_0(980), K_0^*(1430), f_0(1500), \quad (3)$$

with large flavor mixing, just as in the pseudoscalar nonet, i.e. with flavor components  $(u\bar{u}, d\bar{d}, s\bar{s})$  approximately given by

$$\eta', f_0(980) \leftrightarrow (1, 1, 2)/\sqrt{6}, \\ \eta, f_0(1500) \leftrightarrow (1, 1, -1)/\sqrt{3}, \quad (4)$$

close to the flavor singlet or octet respectively and with the parity partners  $\eta'$  and  $f_0(980)$ .

This scalar nonet separates to a good approximation into the singlet  $f_0(980)$  and the octet  $a_0(980)$ ,  $K_0^*(1430)$ ,  $f_0(1500)$ . The octet, within this approximation, fulfills the Gell-Mann–Okubo mass formula and is also consistent with a chiral model with general QCD interaction of the  $\Sigma$  fields. In elastic  $\pi\pi$  scattering and in other channels the cross section shows a broad “background” which extends from below 1000 MeV up to about 1600 MeV or higher, with dips from negative interference with narrow states  $f_0(980)$  and  $f_0(1500)$  (“red dragon”). The PDG has listed here the two states left over so far,  $f_0(600)$  and  $f_0(1370)$ . We have interpreted this “background” as signals from a single broad object  $f_0(1000)$  centered around 1000 MeV with a large width of 500–1000 MeV (according to the  $T$  matrix pole parameters [33, 34]). This “left over state” was taken as the  $0^{++}$  glueball, as its production characteristics followed largely the expectations for a gluonic meson (except for  $J/\psi \rightarrow \gamma\pi\pi$ ). Subsequent studies of various decay rates and relative amplitude phases involving  $f_0(980)$  and  $f_0(1500)$  have confirmed this view [35, 36]; sometimes better experimental data would be desirable. The light scalar objects  $\sigma, \kappa$  are not considered as individual physical particles to be classified into a nonet. The heavier particles  $a_0(1450)$ ,  $f_0(1710)$  could be members of a second nonet, possibly with  $K^*(1950)$  and  $f_0(2020)$ .

There are other approaches which agree on  $f_0(980)$  as being the lightest particle in the nonet. A scheme similar to ours above for the  $q\bar{q}$  nonet with  $f_0(980)$  and  $f_0(1500)$  and mixing like (4) has been proposed [37] based on a quark model with instanton interactions. It prefers though  $a_0(1450)$  over  $a_0(980)$  as nonet partner of  $f_0(980)$ , but there is no prediction on a glueball. The broad enhancements in  $\pi\pi$  and also  $4\pi$  spectra have been interpreted as a consequence of  $\rho$ -exchange in two-body scattering amplitudes [38].

A broad glueball (width about 2 GeV) is found in the mass range 1200–1600 MeV from overlapping  $f_0$  states in a  $K$  matrix analysis of a variety of reactions [42]. The glueball nature of this state has been inferred from its “flavor blind couplings”. Two  $q\bar{q}$  multiplets emerge in the mass range below 1900 MeV including  $f_0(1300)$  and again  $f_0(980)$  as the lightest scalar which now behaves like a flavor octet.

Using results from QCD sum rules a scheme for light scalars has been proposed [39] where a broad isoscalar “ $\sigma$ ” around 1000 MeV and the narrow  $f_0(980)$  are both mixed in equal parts from the broad glueball and a light  $q\bar{q}$  scalar.

Despite various differences in detail, especially the role of the glueball, all these schemes have  $f_0(980)$  as the lightest member of the nonet.

#### Route B: Scalar nonet with $f_0(980)$ and lighter particles

In a second line of thought there is one  $q\bar{q}$  nonet at heavier mass and, in general, a second nonet  $q\bar{q}$  or  $qq\bar{q}\bar{q}$  at lower mass including  $f_0(980)$ . The heavier multiplet includes  $K_0^*(1430)$ ; the isovector candidate in the same mass region is  $a_0(1450)$ . In the isoscalar channel one observes  $f_0(1370)$ ,  $f_0(1500)$  and  $f_0(1710)$ . The scalar glueball is assumed with mass around 1600 MeV as suggested by quenched lattice calculations. Then the glueball and two isoscalar members of the nonet can mix and generate the three observed  $f_0$  states above. Several such mixing schemes have been proposed giving either a larger gluonic component to  $f_0(1500)$  [43] or to  $f_0(1710)$  [44].

The lower mass scalars are now left over. An interesting possibility is the existence of a light nonet including

$$f_0(980), a_0(980), \kappa(850), \sigma(600) \quad (5)$$

(alternatively also  $K^*(1430)$ ). This nonet could be of conventional  $q\bar{q}$  type [45–48] or built from  $qq\bar{q}\bar{q}$  [49–51]. Mesons of this light nonet can also be related to poles in meson–meson scattering amplitudes constructed using chiral symmetry and unitarity [52]. Accepting the existence of  $\sigma$  and  $\kappa$  particles one could have two nonets below 1800 MeV (for reviews, see also [53–55]).

Finally, we should comment on the problem of the  $\sigma$ ,  $\kappa$  poles whose interpretation as particles remains controversial [56, 57]. The evidence has been studied in detail in  $\pi\pi$  scattering within a class of parametrizations which respect chiral symmetry and unitarity [58]. The small scattering length and the rapid increase of the isoscalar  $S$  wave phase shifts with energy required by unitarity yields a pole in the amplitude related to  $\sigma$ . Whether the pole in this parametrization represents a physical particle is not immediately obvious.

In particular, it has been pointed out [59] that final state  $\pi\pi$  interactions calculated within the non-linear sigma model up to two loops “mock up” such a particle: the “ $\sigma$ ” particle is nothing but a convenient parametrization of the correlated two pion exchange. Here we wish to argue that – if these objects are really physical particles – the decay amplitudes should respect the associated flavor symmetry relations which we discuss below.

The aim of our paper is the identification of the lightest scalar nonet and possibly the light scalar glueball. The first step in the next section is a classification of amplitudes in charmless  $B$  decays. We describe an approximation for decays into two pseudoscalar ( $PP$ ) or into a pseudoscalar and a vector particle ( $PV$ ) employing  $U(3)$  flavor symmetry and compare with the recent experimental results; gluonic transitions play an important role. In Sect. 3 we turn to the discussion of scalar particles ( $S$ ) in the final states ( $PS$ ) and ( $VS$ ), which is the main interest of this paper, and we present the corresponding decay amplitudes.

For illustration we compare our formulae with the first experimental data for two different scenarios of the scalar sector and present further predictions. One possible interpretation of the data involves a broad scalar glueball; in Sect. 4 we estimate the total gluonic contributions to  $B$  decays and compare with perturbative calculations. Conclusions follow in Sect. 5. The detailed study of charmless  $B$  decays should help distinguishing the various possibilities outlined above.

## 2 Charmless $B$ decays with $K$ and $K^*(890)$

Our aim is the description of charmless  $B$  decays into scalar particles ( $S$ ) together with particles from pseudoscalar ( $P$ ) and vector ( $V$ ) multiplets,  $B \rightarrow PS$ ,  $B \rightarrow VS$ , including especially the recently observed scalar  $f_0(980)$ . In view of the yet incomplete understanding of the scalar sector and the scarce data we are interested in the leading approximation which describes the main effects. We begin by reconsidering the well studied decays  $B \rightarrow PP$ ,  $B \rightarrow VP$ , especially  $B \rightarrow K\eta'$ ,  $K^*\eta'$ , together with the other final states related by  $U(3)$  symmetry. Subsequently we extend these considerations towards the inclusion of scalar particles.

### 2.1 Approximation for two-body decays

The large branching fraction  $B \rightarrow K\eta'$  confirms the special role of  $\eta'$  in these decays and it has been related [15–18] to the gluon affinity of  $\eta'$ , especially through the QCD axial anomaly which affects only the flavor singlet component. In the factorization approach many two-body decays can be reproduced well but not  $B \rightarrow K\eta'$  [60, 61]. Also, it appears to be difficult to explain the  $K\eta'$  rate entirely by quark final states and the QCD anomaly within a perturbative framework [62]; a factor 2 remains unexplained. An improvement is possible by inclusion of QCD radiative corrections [63] but with considerable uncertainties.

Alternatively, one may introduce a phenomenological flavor singlet amplitude which allows also for non-perturbative effects [18]. This amplitude is added to the dominant penguin amplitudes, the small tree amplitudes and electroweak penguins. Different decays are related by flavor  $U(3)$  symmetry. Recent applications [64, 66] of this scheme to two-body  $B$  decays with strange and non-strange pseudoscalar and vector particles yield a good overall agreement with the data in terms of a few phenomenological input amplitudes.

Here we discuss first the two-body  $B$  decays with  $K$  and  $K^*$  in this way [64, 66] to understand the pattern of the observed rates and then extend the analysis to the scalar sector. For this purpose we restrict ourselves to a simple approximation. In the description of the short distance interaction we keep only the dominant QCD penguin amplitudes  $T_q$  for  $b \rightarrow q\bar{q}s$ ,  $q = u, d, s$  with intermediate virtual gluon and  $T_u = T_d = T_s$  as well as the penguin amplitude with hard gluon radiation (see Fig. 1a,c), while we neglect the electroweak tree diagrams which are CKM

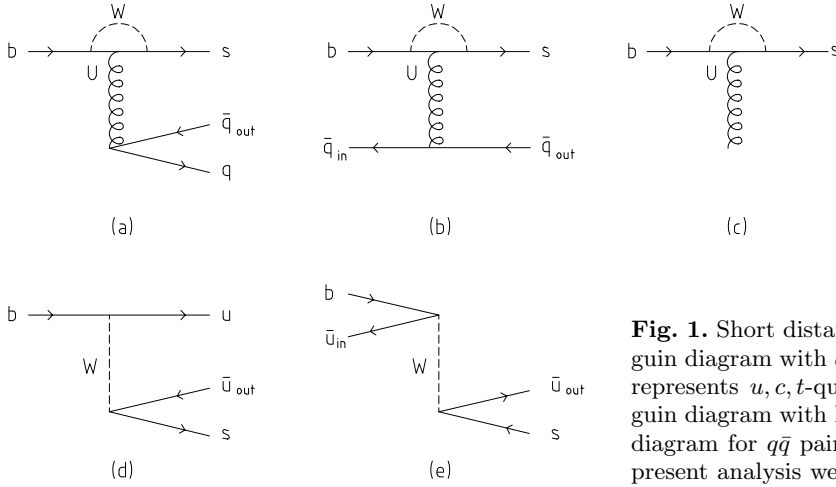


**Fig. 1.** Short distance processes for charmless  $b$  decays: **a** QCD penguin diagram with  $q\bar{q}$  pair production through intermediate gluon ( $U$  represents  $u, c, t$ -quarks) and **b** with spectator annihilation; **c** penguin diagram with hard gluon; **d** electroweak (CKM-suppressed) tree diagram for  $q\bar{q}$  pair production and **e** spectator annihilation. In the present analysis we keep only **a** and **c**

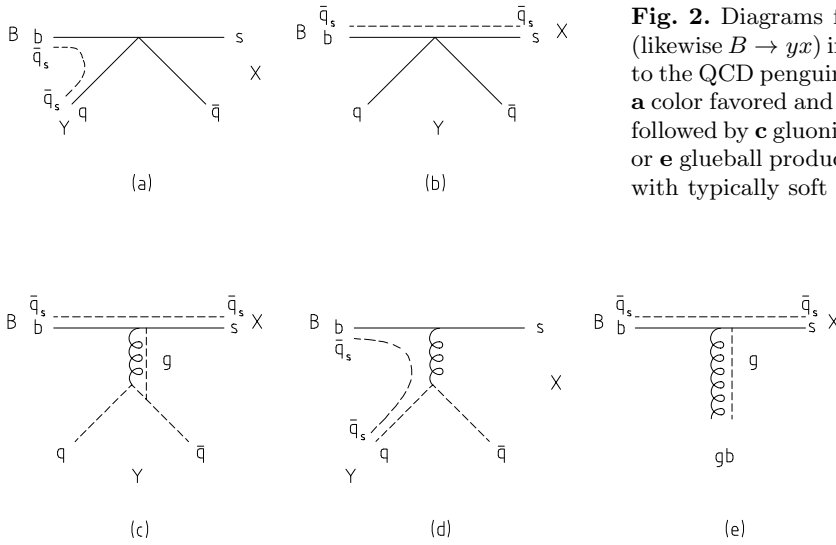


**Fig. 2.** Diagrams for charmless hadronic two-body decays  $B \rightarrow xy$  (likewise  $B \rightarrow yx$ ) into hadrons  $x, y$  from flavor multiplets  $X, Y$  related to the QCD penguin amplitudes of Fig. 1a–c: with  $b \rightarrow s\bar{q}q$  followed by **a** color favored and **b** color suppressed hadron formation; with  $b \rightarrow sg$  followed by **c** gluonic color neutralization and **d**  $q\bar{q}$  color neutralization or **e** glueball production. The dashed lines indicate quarks and gluons with typically soft interactions

suppressed in  $|V_{us}| = 0.22$  (Fig. 1d) as well as the spectator annihilation processes of any kind (Fig. 1b,e) because of the large  $b$ -quark mass.

Concerning the suppression of the tree diagrams we refer to the calculations [20, 22] of decay rates at the quark level including penguin and tree amplitudes. The decays of interest to us are found with relative fractions [22] 22% ( $b \rightarrow u\bar{u}s$ ), 18% ( $b \rightarrow d\bar{d}s$ ) and 15% ( $b \rightarrow s\bar{s}s$ ) of all charmless hadronic  $B$  decays (a total of  $(55 \pm 5\%)$ , the remaining  $\sim 45\%$  correspond to  $b \rightarrow sg$ ). So the non-leading weak decay amplitudes which we neglect here modify the leading result for these rates from penguin amplitudes by about  $\pm 20\%$ ; they become essential, if  $CP$ -violating effects are investigated.

Next we discuss the hadronic two-body decays  $B \rightarrow xy$  with particles  $x, y$  belonging to  $U(3)$  multiplets  $X$  and  $Y$  which are related to the penguin diagrams Fig. 1a,c kept in the present approximation. The  $b \rightarrow s\bar{q}q$  amplitudes in Fig. 1a lead to hadrons either by connection of the spectator quark ( $q_s$ ) in the  $B$  meson with the produced quark  $q$  or with the  $s$ -quark as shown in Fig. 2a,b. The second process is color suppressed as the  $q\bar{q}$  pair produced in a color octet state cannot recombine directly into a hadron; we will

neglect this contribution in the following. The hadronic penguin amplitudes  $p_{xy}^q$  for the decay  $B \rightarrow x(s\bar{q})y(q\bar{q}_s)$  into particles from multiplets  $X$  and  $Y$  in Fig. 2a are then assumed to be proportional within the given multiplet to the amplitudes  $T_q$  in Fig. 1a:

$$\begin{aligned} p_{xy}^q &= A_{s\bar{q}}^x A_{q\bar{q}_s}^y p_{XY}, \\ p_{XY} &= h_{XY} T, \\ T &\equiv T_u = T_d = T_s, \end{aligned} \quad (6)$$

where  $A_{q\bar{q}'}^x$  denotes the flavor coupling  $x \rightarrow q\bar{q}'$  and  $h_{XY}$  a hadronization constant. Likewise there are amplitudes  $p_{yx}^q$  with  $x$  and  $y$  exchanged.

In addition, there is the contribution from the  $b \rightarrow sg$  penguin in Fig. 1c which leads to hadronic final states either by non-perturbative soft color octet ( $g, gg, \dots$ ) or by color triplet ( $q\bar{q}$ ) neutralization of the hard gluon as in Fig. 2c,d.<sup>1</sup> The amplitude in Fig. 2c contributes to the production of a meson  $y$  with flavor singlet  $q\bar{q}$  component (such as the

<sup>1</sup> For a further discussion of these two mechanisms and observable consequences, see, for example, [8].

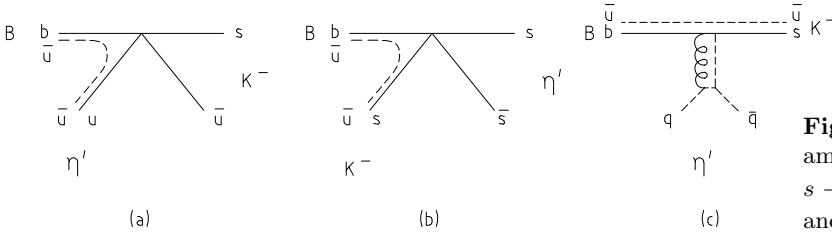


**Fig. 3.** Two-body decay  $B^- \rightarrow K^- \eta'$  with three amplitudes as in Fig. 2a,c: **a** amplitude  $p_{K^- \eta'}^u$  with  $s \rightarrow K^-$ , **b** exchange amplitude  $p_{\eta' K^-}^s$  with  $s \rightarrow \eta'$  and **c** amplitude  $s_{K^- \eta'}$  for gluonic production of  $\eta'$

$\eta'$ ) which we write as

$$s_{xy} = A_{s\bar{q}s}^x (A_{u\bar{u}}^y + A_{d\bar{d}}^y + A_{s\bar{s}}^y) s_{XY}, \quad \text{with} \quad (7)$$

$$s_{XY} = \gamma_{XY} p_{XY}.$$

We take into account this contribution only for the production of scalar and pseudoscalar particles and neglect it for vector particles ( $\omega, \phi$ ). This can be justified by the smaller perturbative transition amplitude with exchange of at least three gluons in the second case as compared to two gluons in the first one; this difference is also considered to be responsible for the large flavor mixing in the pseudoscalar and the small mixing in the vector meson nonet [65]. The smallness of this flavor singlet contribution has also been found in the phenomenological analysis [66]. Furthermore, glueball production is possible through this process (Fig. 2e). The diagram in Fig. 2d has the same quark structure as the one in Fig. 2a and therefore it is not kept independently.

If the two particles belong to two different multiplets then  $p_{yx}^q$  with both decay particles interchanged, i.e. with  $s \rightarrow y$ ,  $q_s \rightarrow x$ , is written as  $\beta'_{XY} p_{xy}^q$ . In case of  $B$  decays into an isoscalar meson with mixed strange and non-strange quark components ( $\eta, \eta', \dots$ ) both amplitudes contribute and interfere, which yields the full amplitude  $p_{xy}^q + \beta_{XY} p_{xy}^{q'}$  where the second term with  $\beta_{XY} = (-1)^L \beta'_{XY}$  refers to the two-particle state with reflected momenta ( $\mathbf{p} \rightarrow -\mathbf{p}$ ) for orbital angular momentum  $L$  [67]. In particular, for  $B \rightarrow VP$  decays there is a relative  $(-)$  sign for the interchange amplitude.

The  $B$  branching ratios are then computed from the superposition of up to three amplitudes depending on the quark structure of  $x$  and  $y$ : the amplitude for the decay  $B \rightarrow x(s\bar{q})y(q\bar{q}_s)$ , the exchange amplitude for the decay  $B \rightarrow y(s\bar{q}')x(q'\bar{q}_s)$  and the gluonic amplitude for decay into an isoscalar meson  $B \rightarrow x(s\bar{q}_s)y(\text{isoscalar } q\bar{q})$ . We have

$$\begin{aligned} \mathcal{B}(B \rightarrow xy) &= |p_{xy}^q + p_{yx}^{q'} + s_{xy}|^2 \\ &= |h_{XY}|^2 |A_{s\bar{q}}^x A_{q\bar{q}_s}^y T_q + A_{s\bar{q}'}^y A_{q'\bar{q}_s}^x \beta_{XY} T_{q'}| \end{aligned}$$

$$+ A_{s\bar{q}s}^x \sum_{q''} A_{q''\bar{q}''}^y \gamma_{XY} T|^2, \quad (8)$$

with the produced quarks  $q, q', q''$ . The decay  $B^- \rightarrow K^- \eta'$  where all three amplitudes contribute is shown in Fig. 3. For the nonets of pseudoscalar, vector and scalar mesons considered here we list the relevant parameters and some notation in Table 1.

## 2.2 Decays into pseudoscalar and vector particles

We apply this simple approximation based on the dominance of penguin diagrams first to the well studied  $B \rightarrow PP$  and  $B \rightarrow VP$  decays. Non-leading diagrams are considered in [64, 66], which are important for the study of  $CP$ -violation effects (absent in our approximation). The relative magnitudes of the tree amplitudes are found there to be of the order of  $\sim 20\%$ .

Without loss of generality we can define  $p_{XY}$  as real in our approximation, whereas  $\beta_{XY}$  and  $\gamma_{XY}$  could be complex in general. However, we assume in the present application also  $\beta_{XY}$  and  $\gamma_{XY}$  to be real, to begin with. Furthermore, we assume an equal recombination probability for the exchanged particles, i.e.  $|\beta_{XY}| = 1$  or  $\beta_{XY} = \pm(-1)^L$ . These simplifications could be relaxed if required by the data. The quark mixing parameters in the pseudoscalar sector are taken from (4), i.e.  $\eta = (u\bar{u} + d\bar{d} - s\bar{s})/\sqrt{3}$  and  $\eta' = (u\bar{u} + d\bar{d} + 2s\bar{s})/\sqrt{6}$ .

Results for  $B \rightarrow PP$  and  $B \rightarrow VP$  decays are given in Table 2, the amplitudes entering (8) in col. 2 and explicitly in col. 3 for  $T_q = 1$  in units of  $p_{PP}$  and  $p_{VP}$  with parameters  $\gamma_{PP}$  and  $\gamma_{VP}$  and  $\beta_{VP} = -1$ . Repeating the calculation with  $\beta_{VP} = +1$  would exchange the roles of  $K^{*+}\eta$  and  $K^{*+}\eta'$  and can therefore be excluded by comparing with the data. The  $B^+$  decay rates are obtained by adjusting in each sector the normalization of  $|p_{XY}|^2$  and by multiplying the amplitude squared in col. 3 with  $|p_{XY}|^2$ . The predictions for  $B^0$  follow by multiplying  $|p_{XY}|^2$  with the ratio  $\tau_{B^0}/\tau_{B^+} = 0.921$  [24].

**Table 1.** Parameters for decays  $B \rightarrow xy$  ( $s \rightarrow x$ ,  $q_s \rightarrow y$ ) for pseudoscalar ( $P$ ), vector ( $V$ ) and scalar ( $S$ ) particles and some special choices in the present analysis

$XY$	penguin	flavor singlet	special choices
$PP$	$p_{PP}$	$s_{PP} = \gamma_{PP} p_{PP}$	
$VP$	$p_{VP}$	$s_{VP} = \gamma_{VP} p_{VP}$	$\beta_{VP} = -1$ , $\gamma_{VP} = \gamma_{PP}$
$PS$	$p_{PS}$	$s_{PS} = \beta_{PS} p_{PS}$	$\beta_{PS} = \pm 1$
		$s_{SP} = \gamma_{SP} p_{PS}$	
$VS$	$p_{VS}$	$s_{VS} = \beta_{VS} p_{VS}$	$\beta_{VS} = -\beta_{PS}$ , $\gamma_{VS} = \gamma_{PS}$

**Table 2.** Branching ratios for  $B^+$  and  $B^0$  decays into pseudoscalar ( $P$ ) and vector ( $V$ ) particles (cols. 4,5) and amplitudes in (8) (col. 2),  $\gamma_{PP}, \gamma_{VP}$  and  $\beta_{VP}$  for gluonic and interchange processes; col. 3:  $T_q, \alpha \equiv p_{VP}/p_{PP}$  set to 1; col. 4:  $\alpha = 0.661$ ,  $\gamma_{PP} = \gamma_{VP} = 0.439$ ,  $\beta_{VP} = -1$ ,  $|p_{PP}|^2 = 20.6 \times 10^{-6}$

$B \rightarrow PP$	amplitudes	$T_q = 1$	$\mathcal{B}_{\text{th}}[10^{-6}]$	$\mathcal{B}_{\text{exp}}[10^{-6}]$
$K^0\pi^+$	$T_d$	1	input $p_{PP}$	$20.6 \pm 1.3$
$K^+\pi^0$	$\frac{1}{\sqrt{2}}T_u$	$\frac{1}{\sqrt{2}}$	10.3	$12.8 \pm 1.1$
$K^+\eta$	$\frac{1}{\sqrt{3}}(T_u - T_s + \gamma_{PP}T)$	$\frac{1}{\sqrt{3}}\gamma_{PP}$	1.3	$3.1 \pm 0.7$
$K^+\eta'$	$\frac{1}{\sqrt{6}}(T_u + 2T_s + 4\gamma_{PP}T)$	$\frac{1}{\sqrt{6}}(3 + 4\gamma_{PP})$	input $\gamma_{PP}$	$77.6 \pm 4.6$
$K^+\pi^-$	$T_u$	1	19.0	$18.2 \pm 0.8$
$K^0\pi^0$	$-\frac{1}{\sqrt{2}}T_d$	$-\frac{1}{\sqrt{2}}$	9.5	$11.2 \pm 1.4$
$K^0\eta$	$\frac{1}{\sqrt{3}}(T_d - T_s + \gamma_{PP}T)$	$\frac{1}{\sqrt{3}}\gamma_{PP}$	1.2	$< 4.6$
$K^0\eta'$	$\frac{1}{\sqrt{6}}(T_d + 2T_s + 4\gamma_{PP}T)$	$\frac{1}{\sqrt{6}}(3 + 4\gamma_{PP})$	71.5	$60.6 \pm 7.0$
$B \rightarrow VP$		$\alpha = 1, \beta_{VP} = -1$		
$K^{*0}\pi^+$	$\alpha T_d$	1	input $\alpha$	$9.0 \pm 1.4$
$K^{*+}\pi^0$	$\frac{\alpha}{\sqrt{2}}T_u$	$\frac{1}{\sqrt{2}}$	4.5	$< 31$
$K^{*+}\eta$	$\frac{\alpha}{\sqrt{3}}(T_u - \beta_{VP}T_s + \gamma_{VP}T)$	$\frac{1}{\sqrt{3}}(2 + \gamma_{VP})$	17.8	$25.9 \pm 3.4$
$K^{*+}\eta'$	$\frac{\alpha}{\sqrt{6}}(T_u + 2\beta_{VP}T_s + 4\gamma_{VP}T)$	$\frac{1}{\sqrt{6}}(-1 + 4\gamma_{VP})$	0.9	$< 12$
$\rho^+K^0$	$\alpha\beta_{VP}T_d$	-1	9.0	$< 48$
$\rho^0K^+$	$\frac{\alpha}{\sqrt{2}}\beta_{VP}T_u$	$-\frac{1}{\sqrt{2}}$	4.5	$4.1 \pm 0.8$
$\omega K^+$	$\frac{\alpha}{\sqrt{2}}\beta_{VP}T_u$	$-\frac{1}{\sqrt{2}}$	4.5	$5.4 \pm 0.8$
$\phi K^+$	$\alpha T_s$	1	9.0	$9.0 \pm 0.9$
$K^{*+}\pi^-$	$\alpha T_u$	1	8.3	$15.3 \pm 3.8$
$K^{*0}\pi^0$	$-\frac{\alpha}{\sqrt{2}}T_d$	$-\frac{1}{\sqrt{2}}$	4.2	$0.4 \pm 1.8$
$K^{*0}\eta$	$\frac{\alpha}{\sqrt{3}}(T_d - \beta_{VP}T_s + \gamma_{VP}T)$	$\frac{1}{\sqrt{3}}(2 + \gamma_{VP})$	16.4	$17.8 \pm 2.0$
$K^{*0}\eta'$	$\frac{\alpha}{\sqrt{6}}(T_d + 2\beta_{VP}T_s + 4\gamma_{VP}T)$	$\frac{1}{\sqrt{6}}(-1 + 4\gamma_{VP})$	0.8	$< 6.4$
$\rho^-K^+$	$\alpha\beta_{VP}T_u$	-1	8.3	$9.0 \pm 2.3$
$\rho^0K^0$	$-\frac{\alpha}{\sqrt{2}}\beta_{VP}T_d$	$\frac{1}{\sqrt{2}}$	4.2	$< 12.4$
$\omega K^0$	$\frac{\alpha}{\sqrt{2}}\beta_{VP}T_d$	$-\frac{1}{\sqrt{2}}$	4.2	$5.2 \pm 1.1$
$\phi K^0$	$\alpha T_s$	1	8.3	$7.8 \pm 1.1$

We compare with branching ratios updated recently for  $B \rightarrow PP$  [63] and  $B \rightarrow VP$  [66] in col. 5.

In a first approximation we adjust only the two penguin amplitudes  $p_{PP}$  and  $p_{VP} \equiv \alpha p_{PP}$  from two rates ( $K^0\pi^+, K^{*0}\pi^+$ ) and set  $\gamma_{XY} = 0$ . Then the overall pattern of the data is reproduced, except for the rates  $K\eta'$  and  $K^*\eta$  which are significantly too large by a factor of up to  $\sim 3$  ( $K^+\eta'$ : 30.9,  $K^0\eta'$ : 28.5,  $K^{*+}\eta$ : 12.0,  $K^{*0}\eta$ : 11.1). This conclusion follows here from flavor symmetry. The neglect of non-leading short distance terms, estimated to amount about 20% cannot account for the discrepancy, which is then attributed to the additional flavor singlet amplitudes  $\gamma_{PP}p_{PP}$  and  $\gamma_{VP}p_{VP}$ .

Predictions for real  $\gamma_P = 0.439$ , determined from  $K^+\eta'$ , are shown in col. 4, and in the  $VP$  sector we chose for simplicity  $\gamma_{VP} = \gamma_{PP}$  (see also the similar results in [64]). At this level of approximation, with expected accuracy of  $\sim 20\%$ , there are no major discrepancies encountered.<sup>2</sup>

<sup>2</sup> There are two predictions with a  $\sim 2.5\sigma$  deviation from the data ( $K^+\eta$  and  $K^{*+}\eta$ ); a better result could be obtained by fitting the three parameters to all branching ratios instead of

Whereas we do not intend to go beyond the present approximations, we may estimate the effect of choosing  $\gamma_{PP}$  complex. Then we find from the  $K\eta$  and  $K\eta'$  rates (Table 2)  $\gamma_{PP} \sim 0.67 \exp(i\varphi_{PP})$ ,  $\varphi_{PP} \sim \pm 67^\circ$ . Using either real or complex  $\gamma_{PP}$  we obtain an estimate of the gluonic part of the  $K\eta', K\eta$  production rate:

$$\begin{aligned} \mathcal{B}(B^+ \rightarrow K^+\eta', K^+\eta)|_{\text{gluonic}} \\ = 3 |\gamma_{PP} p_{PP}|^2 \sim (12 \dots 28) \times 10^{-6}. \end{aligned} \quad (9)$$

We conclude that the main effects are reproduced in each sector by two parameters, the penguin amplitude  $p_{XY}$  and the flavor singlet parameter  $\gamma_{XY}$ ; furthermore we have chosen  $\beta_{VP} = -1$ .

Of particular importance for our further discussion are the large and small rates for  $K\eta'$  and  $K\eta$  respectively and the abundancies of  $K^*\eta'$  and  $K^*\eta$  in reversed order which the model explains after choosing  $\beta_{VP} = -1$ , so far consistent with the data. This is a consequence of the

three only. Alternatively, one may relax the condition for  $\gamma_{PP}$  to be real or the condition  $\gamma_{VP} = \gamma_{PP}$ .

**Table 3.** Dominant contributions for  $B$  decays into scalar ( $S$ ) + pseudoscalar ( $P$ ) or vector ( $V$ ) particles: penguin amplitudes  $p_{XY}$  (normalized to 1 in each sector as in col. 3 of Table 2), exchange and gluonic amplitudes  $\beta_{PS}, \beta_{VS}$  and  $\gamma_{PS}, \gamma_{SP}, \gamma_{VS}$  respectively with scalar mixing angle  $\varphi_S$ ; in brackets the results for  $\sin \varphi_S = 1/\sqrt{3}$  ( $\varphi_S \sim \varphi_P$ ); cols. 3,6: upper sign for  $B^0$ , lower sign  $B^+$

$B^0 \rightarrow$	$B^+ \rightarrow$	normalization to	$B^0 \rightarrow$	$B^+ \rightarrow$	normalization to
$P + S$	$P + S$	$p_{PS}$	$V + S$	$V + S$	$p_{VS}$
$K^+ a^-$	$K^0 a^+$	1	$K^{*+} a^-$	$K^{*0} a^+$	1
$K^0 a^0$	$K^+ a^0$	$\mp \frac{1}{\sqrt{2}}$	$K^{*0} a^0$	$K^{*+} a^0$	$\mp \frac{1}{\sqrt{2}}$
$K^0 f_0$	$K^+ f_0$	$\frac{1}{\sqrt{2}}(1 + 2\gamma_{PS}) \sin \varphi_S$ $+ (\beta_{PS} + \gamma_{PS}) \cos \varphi_S$ $[\frac{1}{\sqrt{6}}(1 + 2\beta_{PS} + 4\gamma_{PS})]$	$K^{*0} f_0$	$K^{*+} f_0$	$\frac{1}{\sqrt{2}}(1 + 2\gamma_{VS}) \sin \varphi_S$ $+ (\beta_{VS} + \gamma_{VS}) \cos \varphi_S$ $[\frac{1}{\sqrt{6}}(1 + 2\beta_{VS} + 4\gamma_{VS})]$
$K^0 f'_0$	$K^+ f'_0$	$\frac{1}{\sqrt{2}}(1 + 2\gamma_{PS}) \cos \varphi_S$ $- (\beta_{PS} + \gamma_{PS}) \sin \varphi_S$ $[\frac{1}{\sqrt{3}}(1 - \beta_{PS} + \gamma_{PS})]$	$K^{*0} f'_0$	$K^{*+} f'_0$	$\frac{1}{\sqrt{2}}(1 + 2\gamma_{VS}) \cos \varphi_S$ $- (\beta_{VS} + \gamma_{VS}) \sin \varphi_S$ $[\frac{1}{\sqrt{3}}(1 - \beta_{VS} + \gamma_{VS})]$
$\pi^- K_{sc}^{*+}$	$\pi^+ K_{sc}^{*0}$	$\beta_{PS}$	$\rho^- K_{sc}^{*+}$	$\rho^+ K_{sc}^{*0}$	$\beta_{VS}$
$\pi^0 K_{sc}^{*0}$	$\pi^0 K_{sc}^{*+}$	$\mp \frac{1}{\sqrt{2}} \beta_{PS}$	$\rho^0 K_{sc}^{*0}$	$\rho^0 K_{sc}^{*+}$	$\mp \frac{1}{\sqrt{2}} \beta_{VS}$
$\eta K_{sc}^{*0}$	$\eta K_{sc}^{*+}$	$\frac{1}{\sqrt{3}}(-1 + \beta_{PS} + \gamma_{SP})$	$\omega K_{sc}^{*0}$	$\omega K_{sc}^{*+}$	$\frac{1}{\sqrt{2}} \beta_{VS}$
$\eta' K_{sc}^{*0}$	$\eta' K_{sc}^{*+}$	$\frac{1}{\sqrt{6}}(2 + \beta_{PS} + 4\gamma_{SP})$	$\phi K_{sc}^{*0}$	$\phi K_{sc}^{*+}$	1

different signs of the exchanged amplitudes in the  $PP$  and  $VP$  multiplets [64, 67], a feature also present in other analyses [62, 63].

### 3 The scalar nonet in $B$ decays

#### 3.1 Branching ratios: expectations and observations

We now turn to the main part of our paper, the study of scalar particle production in  $B$  decays. This is motivated by the remarkably strong signal observed for the scalar meson  $f_0(980)$  by the BELLE [1] (recent update [3]) and BaBar Collaborations [5] in the decay  $B^+ \rightarrow K^+ \pi^+ \pi^-$ , where almost one half of the total rate above background falls into this sub-channel:

$$\mathcal{B}(B^+ \rightarrow K^+ f_0(980); f_0 \rightarrow \pi\pi) \approx 15 \times 10^{-6}; \quad (10)$$

for more details, see Table 4 below. This large fraction for  $K^+ f_0(980)$  is comparable to pseudoscalar decays and three times larger than  $K^+ \rho^0$ . Such a large rate could be taken as a first hint at the gluonic affinity of this meson as well, but it is clear that a more definitive answer requires an analysis similar to the one with  $\eta'$  for scalar particles and on the basis of their flavor classification. Here we assume  $f_0(980)$  to be a member of a  $U(3)$  nonet.

In Table 3 we have written down the amplitudes for the decays  $B \rightarrow PS$  and  $B \rightarrow VS$  in the approximation as above, keeping only the QCD penguin amplitudes ( $p_{PS}, p_{SP}, p_{VS}, p_{SV}$ ) and gluonic amplitudes ( $s_{PS}, s_{SP}, s_{VS}$ ) for the respective multiplets; see Table 1. We denote the states of the scalar nonet by  $a_0, f_0, K_{sc}^*$ , and  $f'_0$ , where the isoscalar states are mixed strange and non-strange components as follows:

$$\begin{aligned} f_0 &= n\bar{n} \sin \varphi_S + s\bar{s} \cos \varphi_S, \\ f'_0 &= n\bar{n} \cos \varphi_S - s\bar{s} \sin \varphi_S, \end{aligned} \quad (11)$$

with  $n\bar{n} = (u\bar{u} + d\bar{d})/\sqrt{2}$  and mixing angle  $\varphi_S$ . For a given nonet of scalar states Table 3 predicts the corresponding pattern of decay rates in terms of these parameters.

For the  $PS$  decays the parameters are the normalization of the penguin amplitude  $p_{PS}$  and  $\gamma_{PS}, \gamma_{SP}, \beta_{PS}$  and for  $VS$  decays the normalization  $p_{VS}$  and  $\gamma_{VS}, \beta_{VS}$ . According to our experience with the  $PP$  sector we may assume in the beginning real parameters  $\beta, \gamma$  and an equal recombination probability for exchanged processes and therefore restrict ourselves to  $|\beta_{PS}|^2 = 1$ . Furthermore, we assume, as in the case of pseudoscalars, that the replacement of one pseudoscalar by one vector meson keeps the parameters  $\gamma, \beta'$  unaltered and therefore we choose

$$\beta_{PS} = \pm 1, \quad \gamma_{VS} = \gamma_{PS}, \quad \beta_{VS} = -\beta_{PS}, \quad (12)$$

where the opposite sign for  $\beta_{VS}$  comes from the spin factor  $(-1)^L$ .

Next we ask whether besides the very clear signal of  $f_0(980)$  there is any evidence for production of other scalars in the data from BELLE (see [1] and the recent update, still preliminary, with higher statistics [3]) and BABAR [5].

#### $K_0^*(1430)$

A higher mass  $K_0^*$  has been seen by BELLE and by BaBar (BaBar quotes “higher  $K^*$ ” which includes higher spin states in this mass range) with rates reproduced in Table 4. Note the considerable difference in the two solutions by BELLE.

#### $f_0(1500)$ and broad “background” in $K\bar{K}$ and $\pi\pi$

In the first publications by BELLE [1, 2] there was a broad low mass enhancement in the  $K^+ K^-$  and  $K^0 \bar{K}^0$  mass

**Table 4.**  $B$  decays into scalars measured by BELLE [3] and BABAR [5] showing statistical and systematic as well as model errors

$\mathcal{B}(B^+ \rightarrow K^+ f_0(980))$	$(10.3 \pm 1.1^{+1.0+0.2}_{-0.9-1.9}) \times 10^{-6}$	[3]
$\times \mathcal{B}(f_0 \rightarrow \pi^+ \pi^-)$	$(9.2 \pm 1.2 \pm 0.6^{+1.2}_{-1.9} \pm 1.6) \times 10^{-6}$	[5]
$\mathcal{B}(B^+ \rightarrow K_0^{*0}(1430)\pi^+)$	$(25.0 \pm 1.6^{+2.4+0.0}_{-2.1-1.5}) \times 10^{-6}$	[3] Fit $C_0/I$
$\times \mathcal{B}(K_0^{*0} \rightarrow K^+ \pi^-)$	$(6.00 \pm 0.84^{+0.58+0.33}_{-0.52-0.43}) \times 10^{-6}$	[3] Fit $C_0/II$
	$(25.1 \pm 2.0 \pm 2.9^{+9.4}_{-0.5} \pm 4.9) \times 10^{-6}$	[5]
$\mathcal{B}(B^+ \rightarrow K^+ f_0(1500))$	$(18.5 \pm 0.5) \times 10^{-6}$	[3] Fit $B_0/I$
$\times \mathcal{B}(f_0 \rightarrow K^+ K^-)$	$(1.3 \pm 0.2) \times 10^{-6}$	[3] Fit $B_0/II$

spectra without any further structure. The recent preliminary results [3], show a qualitatively different picture: there is a sharper peak at 1500 MeV in the  $K^+K^-$  mass spectrum, whose mass and width agree with  $f_0(1500)$ , above a broad bump (“background”). In the  $\pi^+\pi^-$  mass spectrum a broad “background” can be seen as well; however, there is no comparable peak at 1500 MeV which at first makes the identification with  $f_0(1500)$  difficult in view of the known branching ratio  $\mathcal{B}(f_0(1500) \rightarrow K\bar{K})/\mathcal{B}(f_0(1500) \rightarrow \pi\pi) = 0.241 \pm 0.028$  [24] based on the measurements [68, 69]. We will argue below that the identification with  $f_0(1500)$  and its branching ratio is possible if the constructive and destructive interferences, respectively, with the “background” are taken into account. In the  $K^+K^-$  channel BELLE quotes for the resonance rate in two solutions  $B_0/I$  and  $B_0/II$  the quite different fractions 60.8% or 4.4% of the charmless  $K^+K^+K^-$  final state from which we derive (with the errors from the fractions) the numbers in Table 4.

### $f_0(1370)$

Belle [3] also quotes the fractions of a small enhancement near 1300 MeV in  $\pi^+\pi^-$  as  $f_X(1300)$  which could be a signal from  $f_0(1370)$ .

### $\kappa(850)$

The existence of this state with parameters determined by the E791 Collaboration [70] (mass 797 MeV, width 410 MeV) could not be verified by BELLE [3]. If a resonance is fitted it would have the much larger width of 2.27 GeV. The best description of the decay  $B^+ \rightarrow K^+\pi^+\pi^-$  by BELLE includes a broad background in  $K\pi$  with constant phase.

### $\sigma(600)$

One may ask also whether there is any evidence for the  $\sigma(600)$  particle which is seen in some experiments as a peak near the  $\pi\pi$  threshold. The recent BELLE data [3] do not show any peak below the  $\rho$  meson above background whereas the statistics in BaBar is too low to make definite statements. It would be interesting to have some limits or

estimates of the  $B$  branching fractions into these hypothetical mesons  $\sigma$  and  $\kappa$  to be compared with the  $f_0(980)$  branching fraction.

### $a_0(980)$

An important state in scalar spectroscopy is the  $a_0(980)$  which directly measures the penguin amplitude within the scheme of Table 3. A possible decay mode is  $a \rightarrow K\bar{K}$ , which yields a peak just above  $K\bar{K}$  threshold. It is interesting to note that the decay  $B^0 \rightarrow K^+K^-K^0$  studied by BELLE [2] clearly shows such a threshold enhancement near 1000 MeV in  $K^+K^0$  and  $K^-K^0$ , which could be due to  $a_0(980)$  decay. However, there is a large background in this region from non- $B$  decays and there is no claim for observation of  $a_0(980)$  by the BELLE Collaboration.<sup>3</sup> A determination through the decay mode  $a_0(980) \rightarrow \eta\pi$  would be interesting, also for the heavier  $a_0(1450)$ . Such studies would decide whether the nonet partner of  $f_0(980)$  is  $a_0(980)$  or  $a_0(1450)$ .

The above list suggests the observation of scalar states heavier than  $f_0(980)$  whereas there is no clear evidence yet for the observation of the states of lower mass. This is along Route A, which we discuss next.

## 3.2 Comparison with heavy nonet scheme

In this scheme  $f_0(980)$  is the lightest member of the nonet. Specifically, in our version [32] the members are as in (3) and in addition there is a broad glueball. The scheme [37] is similar, with preference for  $a_0(1450)$  but without glueball. In both schemes  $f_0(980)$  and  $f_0(1500)$  are mixed as given by (4).

We begin with a discussion of the production of  $f_0(1500)$ . The peak in the  $K^+K^-$  mass spectrum and the lack of a signal in  $\pi^+\pi^-$  finds a natural interpretation in the quark structure (4) with the negative sign between non-strange and strange components [32, 37] together with the glueball interpretation of the background [32]. This negative relative sign transfers into the decay amplitudes of  $f_0 \rightarrow K\bar{K}$  on one side and  $f_0 \rightarrow \pi\pi$  or  $f_0 \rightarrow \eta\eta$  on the other side, whereas for the glueball the decay amplitudes have the same sign for all pseudoscalar pairs. Therefore,

<sup>3</sup> We thank A. Garmash for clarification of this point.



**Table 5.** Parameters for resonances and their production amplitudes used in the description of the  $\pi\pi$  and  $K\bar{K}$  mass spectra in (13)

state	mass [GeV]	width [GeV]	$T(\pi^+\pi^-)$	$T(K^+K^-)$
$f_0(980)$	0.99	0.05	$c_2 = 5.00 e^{0.1i\pi}$	$c_2 = 2.75 e^{0.1i\pi}$
$f_0(1500)$	1.48	0.10	$c_3 = 1.35 e^{1.50i\pi}$	$c_3 = 0.34 e^{0.75i\pi}$
gb	1.15	0.70	1	1

if the interference  $f_0(1500)$ –background is constructive for  $K\bar{K}$  we expect it to be destructive in  $\pi\pi$ . We recall that such a difference has been observed already in the channels  $\pi\pi \rightarrow K\bar{K}$  and  $\pi\pi \rightarrow \eta\eta$  in their interference with the broad background according to our earlier analysis [32].

In order to check the validity of this proposal quantitatively, for the given decay ratio of  $f_0(1500)$  into  $K\bar{K}$  and  $\pi\pi$  we compare the data with a simple parameterization of the decay amplitudes in terms of  $f_0(980)$ ,  $f_0(1500)$  and the broad background which we interpret as glueball (gb). The new feature of this fit in comparison to the original BELLE work [3] is the common description of both the  $\pi\pi$  and  $K\bar{K}$  channels and the inclusion of a background amplitude in both channels with a phase according to a broad resonance. A more complete analysis should provide a fit of the two-dimensional Dalitz plot density taking into account the interferences of resonances in the crossed channels. Here we are only interested in the low mass region, below 1700 MeV. In this region, we may neglect the small contribution from crossed channel resonances in  $K^+\pi^+\pi^-$  ( $K^*$ ); in  $K^+K^-$  there seems to be some additional contribution below the low mass enhancement which could come from charmed meson sources in the crossed channel or some other background.

In any case, we consider only single channel amplitudes (with interactions in  $\pi^+\pi^-$  or  $K^+K^-$ ) which we describe as a superposition of the three resonance contributions. The spectrum in the pair mass  $m$  is then given by

$$\frac{d\Gamma}{dm} = |c_1|^2 qp |T_{\text{gb}} + c_2 T_{f_0} S_{\text{gb}} + c_3 T_{f'_0} S_{\text{gb}}|^2 \quad (13)$$

$$T_a = \frac{m_a \Gamma_a}{m_a^2 - m^2 - im_a \Gamma_a (1 + G_a(m))}, \quad (14)$$

$$a = \text{gb}, f_0, f'_0,$$

$$S_{\text{gb}} = e^{2i\delta_{bg}}; \quad T_{\text{gb}} = |T_{\text{gb}}| e^{i\delta_{bg}}. \quad (15)$$

The superposition of a narrow resonance with a broad background we describe by the rotation of the resonance term in the complex plane with the background  $S$  matrix,  $S = e^{2i\delta_{bg}}$ , which is consistent with unitarity in the elastic region as is well known; here we also apply it in the inelastic region. In (13)  $q$  is the hadron momentum in the  $h^+h^-$  restframe and  $p$  the momentum of the  $h^+h^-$  pair in the  $B$  restframe.

The resonances included here cannot be given by a simple Breit–Wigner form in the considered mass range, because of the distortion by inelastic  $K\bar{K}$ ,  $\eta\eta$  and  $4\pi$  ( $\rho\rho$ ) thresholds. In our present exploratory study we do not attempt a full treatment of unitarity effects of the coupled

channel system; rather we allow for an energy dependent width which takes into account the  $K\bar{K}$  threshold. As we are unable to fix the shape function  $G_a(m)$  in our fitting of projected densities we choose, for definiteness, a form which ties the amplitude at energies  $> 1.6$  GeV back to the original resonance circle and is otherwise adjusted to give a reasonable representation of the mass spectra. For  $f_0(980)$  and the glueball (gb) we chose

$$K\pi\pi : \quad (16)$$

$$G_a(m) = \Theta(m - 2m_K) \varepsilon_\pi x \exp(-(m/m_1)^{11}),$$

$$K\bar{K}K : \quad (17)$$

$$G_a(m) = \Theta(m - 2m_K) \varepsilon_K x \exp(-(m/m_2)^{11.5}),$$

with  $x = \sqrt{1 - 4m_K^2/m^2}$  and parameters  $\varepsilon_\pi = 0.9$ ,  $\varepsilon_K = 2.5$ ,  $m_1 = 1.28$  GeV,  $m_2 = 1.37$  GeV. For  $f_0(1500)$ , further away from the important thresholds, we put  $G_a(m) = 0$ . The resonance parameters and production amplitudes are taken as in Table 5. Concerning the glueball parameters we note that the elastic  $\pi\pi$  scattering amplitude in the intermediate energy region around 1 GeV can be represented by a superposition of  $T$ -matrix poles from  $f_0(980)$  and a broad state with mass near 1000 MeV and a width of 500–1000 MeV as has been known since long [33, 34]. More recent analyses prefer a slightly higher mass in the region 1200–1600 MeV for this broad state by fitting to a larger number of channels [42].

The amplitudes were obtained by adjusting the parameters “by eye” to investigate the result from superimposing the three resonances with relative phases, where we kept the branching ratio of  $f_0(1500)$  at the value suggested by the PDG (i.e.  $K^+K^-/\pi^+\pi^- = 3/4 \times 0.241$ ), and to describe the data at least qualitatively. We do not include the production of the  $\rho$  meson which is clearly present [3]. The results with these parameters are shown in Figs. 4 and 5 in comparison with the BELLE data.

We note that the relative phase between  $f_0(1500)$  in  $\pi\pi$  and  $K\bar{K}$  is  $0.75\pi$ , close to the expected value  $\pi$  for a near octet resonance; see Table 5. This phase difference causes the peak and dip in  $K^+K^-$  and  $\pi^+\pi^-$  respectively which we consider as an important further confirmation of the near octet nature of this meson, which does not allow for a sizable glueball admixture (the glueball would contribute with the same sign to both particle pairs; see also [32, 36]).

In our parameterization the phases for  $f_0(980) \rightarrow \pi^+\pi^-$  and  $f_0(980) \rightarrow K^+K^-$  decays are about the same, but these phases are less well determined by the data. Note that the relative phase between both  $f_0(980)$  amplitudes is about zero relative to the background in Table 5. The glueball amplitude representing the broad background has

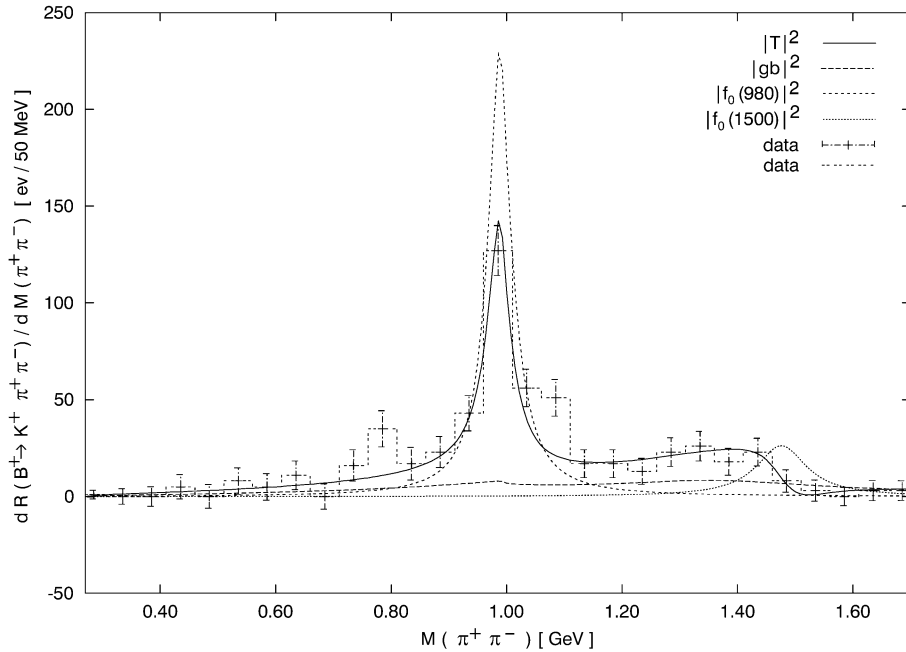


**Fig. 4.**  $\pi^+\pi^-$  mass spectrum in  $B$  decays as measured by BELLE [3] in comparison with a model amplitude  $|T|^2$  of the coherent superposition of  $f_0(980)$ ,  $f_0(1500)$  and a glueball (gb) forming the broad background. Also shown are the individual resonance terms  $|T_R|^2$ . The background (gb) in this fit interferes destructively with both  $f_0(980)$  and  $f_0(1500)$  consistent with the model (see (4) and (13))

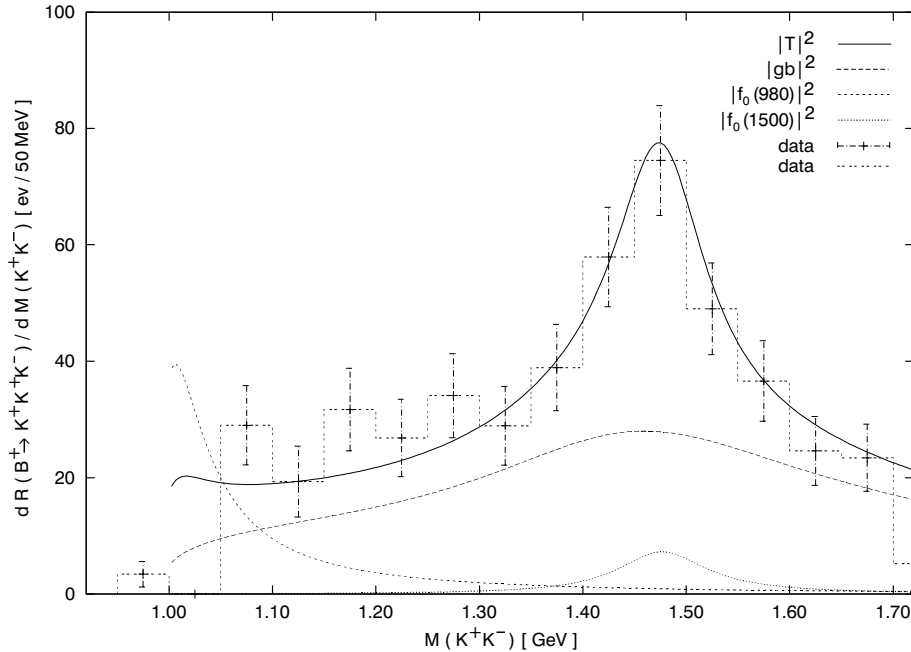


**Fig. 5.**  $K^+K^-$  mass spectrum in  $B$  decays as measured by BELLE [3] in comparison with the model amplitude, see Fig. (4). Here  $f_0(1500)$  interferes constructively with the background

phase  $\delta_{\text{gb}} \approx \pi/2$  near the pole position around 1000 MeV. Therefore the interference with  $f_0(980)$  is *destructive* because of the phase factor  $S \approx e^{i\pi}$  in (13). This is well known for elastic  $\pi\pi$  scattering where  $f_0(980)$  produces a dip instead of a peak in the mass spectrum. In our present fit the small background does not produce a dip but it reduces the size of the  $f_0(980)$  peak in Fig. 4; however, the phase is not so well determined and a constructive interference cannot be excluded. This requires a study of the lineshape with higher accuracy. Such a phenomenon is met with also in the decay  $J/\psi \rightarrow \phi\pi\pi$  [72] where the interference of  $f_0(980)$  with the background is destructive. This is derived from the asymmetric shape of  $f_0(980)$ .

Our description also reproduces approximately the small enhancement near 1300 MeV which is generated by the interference of all three states. On the other hand, it has been interpreted by BELLE as to be due to  $f_0(1370)$ . Whether  $f_0(1370)$  really exists as a particle is still controversial. The PDG does not confirm any branching ratio. If the measurement of the decay ratio  $\mathcal{B}(f_0(1370) \rightarrow K\bar{K})/\mathcal{B}(f_0(1370) \rightarrow \pi\pi) = 0.46 \pm 0.15 \pm 0.11$  [71] is taken for granted, one should see in  $B$  decays in both channels an effect of size comparable to  $f_0(1500)$ . The  $K^+K^-$  spectrum does not provide immediate evidence for such a situation.

Finally, we determine the decay rates for the resonances studied and compare with our expectations from Table 3. From our analysis we obtain the number of events for each

**Table 6.** Decay branching ratios for resonant contributions in  $B^+ \rightarrow K^+\pi^+\pi^-$  and  $B^+ \rightarrow K^+K^+K^-$  for masses  $m < 1.72$  GeV from our analysis using the branching ratio equivalents of  $0.05417 \times 10^{-6}$  and  $0.03657 \times 10^{-6}$  per event (as concluded from [3]) for both final states respectively

channel	gb [ $10^{-6}$ ]	$f_0(980)$ [ $10^{-6}$ ]	$f_0(1500)$ [ $10^{-6}$ ]
$\pi^+\pi^-$	7.4	19.3	4.3
$\pi\pi$	11.1	29.0	6.5
$K^+K^-$	10.1	2.1	0.70
$K\bar{K}$	20.2	4.2	1.4
all		-33.2	20.3

state (the area under the curves for our three states  $|T_a|^2$  in Figs. 4 and 5). Relating the total event numbers in the two channels with the corresponding branching ratios for charmless decays we arrive at the numbers in Table 6. In order to obtain the total rates we added for  $f_0(980)$  the observed decays in  $\pi\pi$  and  $K\bar{K}$ . In the case of  $f_0(1500)$  a complete sequence of branching ratios is not available from the PDG. If we use the ratios determined by the PDG [24] and estimate the ratio  $\mathcal{B}(f_0 \rightarrow 4\pi)/\mathcal{B}(f_0 \rightarrow 2\pi) \approx 1.7$  from their listing we obtain the following estimate for the branching ratios:

$$f_0(1500) : 4\pi (54.2\%), 2\pi (32.0\%), K\bar{K} (7.8\%), \\ \eta\eta (4.2\%), \eta\eta' (1.8\%).$$

From the  $2\pi$  decay we obtain the branching ratios of Table 6.

We note that our result for  $f_0(980) \rightarrow \pi^+\pi^-$  is about twice as large as in Table 4, whereas our result for  $f_0(1500) \rightarrow K^+K^-$  is smaller by the same amount compared to the Fit  $B_0/II$  and much smaller than the Fit  $B_0/I$  in Table 4. Note that in the case of  $f_0(1500)$  we fit the  $\pi\pi$  spectrum as well with the  $K\bar{K}/\pi\pi$  ratio kept fixed (at PDG value) and the large rate of Fit  $B_0/I$  seems to be excluded.

If we had taken the fit results by BELLE on  $f_0(980)$  and  $f_0(1500)$  (Fit  $B_0/II$ ) instead of ours in Table 6 we would have obtained the corresponding rates  $17 \times 10^{-6}$  and  $33 \times 10^{-6}$  (instead of  $33.2 \times 10^{-6}$  and  $20.3 \times 10^{-6}$ ). The different results may come partly from a different treatment of the phases, especially our moving background phase; we also remark that our analysis is using an approximation by working only with projections. We estimate that the present numbers for the rates have a model uncertainty by about a factor of two.

Finally, we compare our results with the expectations from Table 3 based on symmetry relations for the nonet. We derive the predictions using the mixing angle  $\sin \varphi = 1/\sqrt{3}$  as in our model [32] and in [37]. We are using the simplifications motivated by the experience with pseudoscalars as outlined in the last subsection. We assume real  $\gamma_{PS}$  and restrict ourselves to  $\beta_{PS} = \pm 1$ . Then we can use the rates for  $f_0 \equiv f_0(980)$  and  $f'_0 \equiv f_0(1500)$  to determine the two parameters  $|p_{PS}|^2$  and  $\gamma_{PS}$ . The result for  $|p_{PS}|^2$  may then be compared with the measurement of the  $K_0^*(1430)\pi$  rate. We allow for both signs of  $\beta_{PS}$  and obtain for each case two solutions from the predictions for the rates following

**Table 7.** Parameters  $|p_{PS}|^2$  (in units of  $10^{-6}$ ) and  $\gamma_{PS}$  in the decay of  $B$  into scalar particles using the symmetry relations in Table 3 and the total branching ratios for  $a_0$ ,  $f_0 \equiv f_0(980)$  and  $f'_0 \equiv f_0(1500)$  from Table 6. There are two solutions for each value of  $\beta_{PS}$ ; further predictions of branching ratios (in units of  $10^{-6}$ ) using for  $K^*(890)$ :  $\gamma_{VS} = \gamma_{PS}$  and  $\beta_{VS} = -\beta_{PS}$  and  $p_{VS}/p_{PS} = 0.437$ ; Sol. 2 excluded, see text

Sol.	$\beta_{PS}$	$ p_{PS} ^2$	$\gamma_{PS}$	$K^0 a_0^+$	$K^{*+} f_0$	$K^{*+} f'_0$	$K^{*0} a_0^+$
1	+1	32.0	-1.38	32.0	13.2	1.8	14.0
2	+1	234.	-0.51	-	-	-	-
3	-1	11.0	1.33	11.0	55.4	2.8	4.8
4	-1	42.1	-0.30	42.1	9.9	0.6	18.4

from Table 3 (amplitudes in brackets) and these results are presented in Table 7.

With  $|\beta_{PS}| = 1$  we can compare these results for  $|p_{PS}|^2$  directly to the rate for  $B^+ \rightarrow K_0^{*0}(1430)\pi^+$  according to Table 3. Correcting the numbers in Table 4 for neutral decays one finds for  $K_0^{*0}\pi^+$  rates of about  $38 \times 10^{-6}$  or  $9 \times 10^{-6}$ . Then we can exclude our Sol. 2 in Table 7 whereas Sol. 1 and 4 are near the Fit  $C_0/I$  in Table 4 and Sol. 3 near the Fit  $C_0/II$ . A more detailed investigation of the Dalitz plot densities could possibly distinguish between Solutions  $C_0/I$  and  $C_0/II$ . Another test is possible through measurement of the  $K^0 a_0^+$  decay which is given directly by  $|p_{PS}|^2$ .

We note that Sol. 4 in Table 7 has similar parameters to the pseudoscalar amplitudes  $\beta_{PP} = 1$  and  $\gamma_{PP} = 0.44$ , except for their opposite sign. On the other hand, Sol. 1 and 3 have a three times larger gluonic amplitude which would not be theoretically expected. If we had taken the BELLE Fit results instead of ours in Table 6 we would have obtained the numbers, corresponding to Sol. 4,  $|p_{PS}|^2 = 30.5 \times 10^{-6}$  and  $\gamma_{PS} = -0.20$ .

In any case, the results obtained are not in contradiction with the suggested scalar nonet of heavier particles along Route A. Actually, our specific approach [32] with nonet (3) and (4) and a broad glueball explains naturally the new observations from  $B$  decays. Further results concern the predictions for production of  $a_0$  and of scalars together with vector mesons, especially  $f_0$ ,  $f'_0$ . These predictions are shown also in Table 7 for the three remaining solutions. Again we make the simplified choices motivated by the experience with the pseudoscalars, as outlined in the previous subsection, and assume  $\gamma_{VS} = \gamma_{PS}$  and  $\beta_{VS} = -\beta_{PS}$  (the opposite sign for  $\beta_{VS}$  comes from the spin factor  $(-1)^L$ ); also we take  $p_{VS}/p_{PS} = 0.661$ . Then we expect a much smaller rate for  $K^* f_0(1500)$  than for  $K^* f_0(980)$ . The rate  $K^{*0} a_0^+$  determines directly the normalization  $|p_{VS}|^2$ . These measurements will provide further important tests of our picture.

### 3.3 Comparison with light nonet scheme

In this approach  $f_0(980)$  falls into the same nonet with  $a_0(980)$  and also with  $\sigma(600)$  and  $\kappa(850)$  whose existence are still under debate. If this nonet is built from  $q\bar{q}$  states

**Table 8.** Rates for some channels with scalars assuming  $f_0(980)$  in a nonet with  $\sigma(600)$  and  $\kappa(850)$  (mixing angle  $\varphi_S = 0$ ) and amplitudes (in units of the penguin amplitudes  $p_{PS}$ ,  $p_{VS}$ ) for two scenarios with different gluonic component  $\gamma_{PS}$ , using  $\beta_{PS} = \pm 1$ . For  $K^*$  decays we take  $\beta_{VS} = -\beta_{PS}$ ,  $\gamma_{VS} = \gamma_{PS}$  and  $p_{PS}/p_{VS} = 0.661$ . The  $K^+\kappa^0$  and  $K^0a_0^+$  rates equal  $|p_{PS}|^2$

$B^+ \rightarrow$	$K^+ f_0$	$K^+ \sigma$	$K^0 a_0^+$	$\pi^+ \kappa^0$	$K^{*+} f_0$	$K^{*+} \sigma$
amplitude	$\beta_{PS} + \gamma_{PS}$	$\frac{1}{\sqrt{2}}(1 + 2\gamma_{PS})$	1	$\beta_{PS}$	$\beta_{VS} + \gamma_{VS}$	$\frac{1}{\sqrt{2}}(1 + 2\gamma_{VS})$
Scenario I :	$\gamma_{PS} = 0$					
rate [ $10^{-6}$ ]	15.	7.5	15.	15.	6.5	3.2
Scenario II :	$\gamma_{PS} = -0.5$					
rate [ $10^{-6}$ ]	15.	$\beta_{PS} = +1$ 0.	60.	60.	59.0	0.
rate [ $10^{-6}$ ]	15.	$\beta_{PS} = -1$ 0.	6.7	6.7	0.7	0.

with mixing as in (11) we can apply the same discussion as before and explore the symmetry relations of Table 3. In case of a  $qq\bar{q}\bar{q}$  model additional degrees of freedom may come in, which we do not consider here. As emphasized in the beginning of this section, there are not yet any definitive observations of these light scalars in  $B$  decays, as they exist for the heavier scalars, nor are there any limits for branching ratios. Therefore we only indicate some possible scenarios to stress the potential of  $B$  decay studies also for these light scalars.

In this case only the rate for  $B^+ \rightarrow K^+ f_0(980)$  is available which we take from (10). A natural choice is the mixing angle  $\varphi_S = 0$  which, according to (11), corresponds to  $f_0(980)$  being a pure strange and  $\sigma$  a pure non-strange state. The decay amplitudes follow from Table 3 and are listed for a few decay channels in Table 8.

The simplest choice is to assume production without gluonic processes, i.e.  $\gamma_{PS} = 0$  (Scenario I) We assume again  $|\beta_{PS}| = 1$ , as in the previous discussions of pseudoscalar and scalar sectors. Then, with the  $f_0$  rate as input we can predict the other states of the multiplet. One finds that in this case the  $K\sigma$  rate is 1/2 of the  $Kf_0$  rate and equal to the  $K\kappa$  rate. This looks rather large for  $\sigma$  in view of the first results [3].

We therefore also consider another Scenario II where we introduce a gluonic coupling of  $f_0$  so as to cancel the  $K\sigma$  decay. In this case the sign of  $\beta_{PS}$  matters, and we obtain for  $K\kappa$  either  $60 \times 10^{-6}$  or  $6.7 \times 10^{-6}$  where the first choice can presumably be excluded from the data [3]. Furthermore, we present some predictions for decays with the vector meson  $K^*$ . Again, the measurement of the  $a_0$  rate would be very useful as it fixes the normalizations for the  $PS$  and  $VS$  multiplets. We conclude that a measurement of the rates for  $\sigma$  and  $\kappa$  will be important for the discussion of their existence, their classification and their production mechanism.

### 3.4 Total rate for gluonic decays

Next we compare the gluonic production rates for  $f_0$ ,  $f'_0$  and  $\eta$ ,  $\eta'$  with the total rate  $b \rightarrow sg$  in (1). CLEO [11] has measured the inclusive non-charm decay  $\mathcal{B}(B \rightarrow \eta' +$

$X) = (6.2^{+2.1}_{-2.6}) \times 10^{-4}$ , where the signal refers to the region  $2.0 < p_{\eta'} < 2.7$  GeV of the  $\eta'$  momentum. Identifying the non-charm rate with  $X_s$  according to the SM and adding the exclusive  $\eta'K$  rate we obtain the inclusive rate  $\mathcal{B}(B \rightarrow \eta' + X_s) \sim 7.0 \times 10^{-4}$ , so the ratio of the total inclusive  $\eta'X_s$  over the exclusive  $\eta'K$  rate is  $R_{\eta'}(\text{incl/excl}) \approx 9$ . We take the gluonic part  $3|\gamma_{PS}p_{PS}|^2$  as in (9) whereas for scalars we find from Table 7 the corresponding result in the range  $(11 \dots 182) \times 10^{-6}$  with preference for the lowest value. Then we find for the fully inclusive contribution of these decays after multiplication with  $R_{\eta'}(\text{incl/excl})$

$$\mathcal{B}(B \rightarrow \eta, \eta', f_0, f'_0)|_{\text{gluonic}} \sim (0.2 \dots 2) \times 10^{-4}, \quad (18)$$

with preference for the lower value. Hence, these decays cannot contribute more than a small fraction of the expected  $b \rightarrow sg$  rate of  $5 \times 10^{-3}$  [20]. We will argue next that glueball production does provide the dominant part of the  $b \rightarrow sg$  decay originating from a genuine hard gluon composing the associated local dimension 5 operator.

## 4 Glueball production in $B$ decays

Besides the observation of the strong  $f_0(980)$  signal there is another interesting clear feature in the  $B$  decays: the presence of a broad low mass  $\pi\pi$  and  $K\bar{K}$  enhancement in  $B^+ \rightarrow K^+\pi^+\pi^-$  and  $B^+ \rightarrow K^+K^-K^+$  with spin  $J = 0$ , observed by the BELLE Collaboration [1–3].

An important signal for the sizable S wave background is the interference with known resonances. The appearance of the  $f_0(1500)$  peak in  $K^+K^-$  on one hand and its disappearance in  $\pi^+\pi^-$  on the other hand can be naturally explained by its constructive and destructive interference with this background, as discussed in the previous section.

This interference is quite pronounced, as in elastic  $\pi\pi$  scattering, where in contrast  $f_0(980)$  and  $f_0(1500)$  appear both as dips in the broad background which we interpreted in our earlier study [32] as destructive interference with the broad glueball (“red dragon”). In the low energy region below 1 GeV we assume that the  $\pi\pi$  amplitudes are moving as in elastic  $\pi\pi$  scattering, at higher masses the movement of the phase is more difficult to predict because of the inelastic

channels. The study of interferences in the Dalitz plot, especially the crossing regions of the known resonances – charmed and uncharmed – with the background and among themselves could eventually show whether the movement of the background phases in the  $\pi\pi$  and  $K\bar{K}$  channels is consistent with an inelastic broad resonance. An open question here is also the relevance of  $f_0(1370)$  in these channels. We argued in [32] that the Breit–Wigner phase motion of an assumed resonance with moderate width at this energy has not been demonstrated clearly enough to require a definite resonance. In a recent analysis of the  $f_0(1370) \rightarrow 4\pi$  channel [73] (as reported in [74]) it was found that in the considered mass range the phase motion was lower than expected from the Breit–Wigner formula so that these data do not support the interpretation of  $f_0(1370)$  as a “normal resonance”.

Besides the prediction of a moving phase the glueball hypothesis has also consequences for the decay fractions into different particles. In order to relate different channels and to obtain an estimate of the total glueball production rate we consider the following decay scheme. The glueball decays first into the various  $q\bar{q}$  pairs with equal amplitude (possibly also into a pair of gluons):

$$gb \rightarrow u\bar{u} + d\bar{d} + s\bar{s} \quad (+gg). \quad (19)$$

The  $gg$  pair could hadronize into two secondary glueballs after the creation of another gluon pair. Our  $0^{++}$  glueball at energies above 1 GeV could decay as  $gb \rightarrow \sigma\sigma$  where  $\sigma(600)$  is considered as the low mass part of the same  $0^{++}$  glueball. Then the main decay process would be  $gb \rightarrow 4\pi$ . In the following we do not consider these decays further here. Each of the  $q\bar{q}$  pairs in (19) recombines with a newly created pair  $u\bar{u}$ ,  $d\bar{d}$  or  $s\bar{s}$ , where  $s\bar{s}$  is produced with amplitude  $S$  ( $|S| \leq 1$ ). In this way the two-body channels  $gb \rightarrow q\bar{q}' + \bar{q}q'$  are opened, but at low energies just pairs of pseudoscalars. They are produced with the probabilities listed in Table 9.

The first row corresponds to  $U(3)$  symmetry ( $S = 1$ ), the second row to arbitrary  $S$  (for numerical estimates we take  $S = 0.8$ );  $\eta, \eta'$  mixing is assumed as above. With increasing glueball mass the  $q\bar{q}$  pairs can decay also into pairs of vector mesons or of other states. The total rates in Table 9 are assumed to remain unaltered but in general “ $\pi\pi$ ” is meant to include  $\rho\rho$  as well above the respective threshold of about 1300 MeV.

We consider first the mass region 1.0–1.7 GeV. In this region the pseudoscalars alone saturate the “ $K\bar{K}$ ” rate in Table 9 as  $K^*\bar{K}$  is forbidden by parity and  $K^*\bar{K}^*$  is kinematically suppressed. Another possible decay is  $\eta\eta$ , contributions from higher mass isoscalars ( $\omega\omega$ ) are only possible at the upper edge of the considered mass interval. The decay  $\eta'\eta'$  is kinematically forbidden.

**Table 9.** Probabilities of pairs of pseudoscalars

$\pi^+\pi^-$	$\pi^0\pi^0$	$K^+K^-$	$K^0\bar{K}^0$	$\eta\eta$	$\eta'\eta'$
2	1	2	2	1	1
2	1	$\frac{1}{2} 1+S ^2$	$\frac{1}{2} 1+S ^2$	$\frac{1}{9} 2+S ^2$	$\frac{1}{9} 1+2S ^2$

In the region 1.1–1.3 GeV, away from the narrow resonances and from the major inelastic thresholds, we may compare the rates into the  $\pi^+\pi^-$  and  $K^+K^-$  channels with the theoretical expectations Table 9. From Figs. 4 and 5 we obtain  $dR/dM(\pi^+\pi^-) \sim 20$  events/50 MeV in the mean and  $dR/dM(K^+K^-) \sim 30$  events/50 MeV, corresponding to  $dR/dM \sim 1 \times 10^{-6}/50$  MeV, in both cases using the  $\mathcal{B}$ -equivalents in Table 6. The glueball fractions in our fits appear at the level of about 1/2 of the experimental data in the mean in both cases in this mass range. Therefore the glueball decay rates in  $\pi^+\pi^-$  and  $K^+K^-$  are approximately equal, within about 20%, consistent with the expectations 2 : 1.6 (for  $S = 0.8$ ) from Table 9.

Above 1600 MeV the two spectra look quite different: whereas the  $K\bar{K}$  spectrum decreases slowly, the  $\pi\pi$  spectrum stays at a low level. This may be explained by assuming that the dominant decay of “ $\pi\pi$ ” in Table 9 proceeds into  $4\pi$  (e.g.  $\rho\rho$ ) states in this mass range.

Next we estimate the total glueball rate. Here we start from our fit result for  $gb \rightarrow K\bar{K}$  in Table 6 referring to the mass interval 1.0...1.72 GeV. Including the contribution from higher masses of about 55% we obtain  $\mathcal{B}(B^+ \rightarrow K^+gb; gb \rightarrow K\bar{K}) \approx 31 \times 10^{-6}$ . This yields an estimate of the lower limit for the exclusive and inclusive branching ratios (correcting for other decay modes without  $gb$  by a factor 2.2 from Table 9 using  $S = 0.8$  by neglecting  $\pi\pi$  decays below 1 GeV and  $\eta\eta'$ ):

$$\mathcal{B}(B^+ \rightarrow gb(0^{++}) + K^+) \gtrsim 70 \times 10^{-6}, \quad (20)$$

$$\mathcal{B}(B^+ \rightarrow gb(0^{++}) + X_s) \gtrsim 0.6 \times 10^{-3}; \quad (21)$$

here we used again the factor 9 from  $K\eta'$  to estimate the fully inclusive rate.

By adding the gluonic pseudoscalar and scalar meson contributions from (18) we estimate the lower limit (neglecting again the  $gg$  decay mode in (19) and choosing Sol. 4 in Table 7) for the total production of observed gluonic scalar and pseudoscalar mesons as

$$\mathcal{B}(B^+ \rightarrow gb(0^{++}) + f_0 + f'_0 + \eta + \eta' + X_s)|_{\text{gluonic}} \gtrsim 0.8 \times 10^{-3}. \quad (22)$$

This lower limit for gluonic production amounts to about 1/2 of the leading order result for the process  $b \rightarrow sg$  in (1) and about 1/6 of the full rate obtained in NLO, so it represents already a sizable fraction of the theoretically derived value. This result supports the expectation that the  $b \rightarrow sg$  rate will be saturated if a few similar processes with other  $J^{PC}$  quantum numbers, especially the  $0^{-+}$  and  $2^{++}$  glueballs, are included.

## 5 Conclusions

The main motivation for our investigation is the search for the lightest glueball which is expected with the  $J^{PC} = 0^{++}$  quantum numbers. To this end it is important to obtain a full understanding of the light scalar sector, i.e. to establish the lightest scalar nonet and its intrinsic mixing.

An important role is played by  $f_0(980)$  which in different classification schemes is either the lightest or the heaviest particle in this nonet (other options are being discussed as well).

In this paper we investigate the potential of  $B$  decays which have the partial decay mode  $b \rightarrow sg$  in the search of gluonic objects. This interest has been triggered by the undisputable observation of  $B \rightarrow K f_0(980)$  with a large rate comparable to the one for pseudoscalar particles. This could imply a large gluonic affinity of this meson or a flavor singlet nature similar to the  $\eta'$ .

For the further investigation of  $B$  decays we suggest a simple approximate scheme for two-body decay rates based on the dominance of penguin amplitudes with an additional gluonic component; for each pair of multiplets there are three amplitudes  $p$ ,  $\gamma p$ ,  $\beta p$ ; the present analysis allows for real  $\gamma$  and  $\beta = \pm 1$ . This model has been tested first in the sector of decays  $B \rightarrow PP$  and  $B \rightarrow VP$  where it corresponds to a simplified version of the previous approach [64]. Because of the (approximate) flavor symmetry of all  $q\bar{q}$  in the decays  $b \rightarrow sq\bar{q}$  all members of the nonet have a common component in the amplitude modified by  $\beta, \gamma$  amplitudes. Exploiting this fact by comparing the rates with the expectations in Table 3 should ultimately disclose the identity of the members of the lightest nonet associated with  $f_0(980)$ .

The choice of the nonet with members  $a_0(980)$ ,  $f_0(980)$ ,  $K_0^*(1430)$ ,  $f_0(1500)$  with  $f_0(980)$  as lightest particle as in [32] and similarly in [37] (with  $a_0(1450)$  preferred) can reproduce the observed phenomena concerning also other scalar particles not yet as well established as  $f_0(980)$ . In particular, there is the remarkable phenomenon of the  $f_0(1500)$  signal in  $K\bar{K}$ , but apparently absent in  $\pi\pi$  despite the four times larger branching ratio. In our analysis this is explained by the constructive and destructive interference respectively with the broad glueball (“background”, “red dragon”). Such a behaviour is expected from the near octet flavor composition of  $f_0(1500)$ . The negative sign between the  $s\bar{s}$  and  $u\bar{u} + d\bar{d}$  component of  $f_0(1500)$  has been found before in inelastic  $\pi\pi$  scattering [32]. If confirmed in the final analysis of the data it would seriously restrict the possible glueball admixtures of  $f_0(1500)$  which yield contributions of equal sign to  $\pi\pi$  and  $K\bar{K}$  decay amplitudes.

An important role in this classification is played by  $a_0(980)$  as the lightest isovector particle which directly determines the penguin amplitude  $p$  and therefore the overall normalization within one multiplet. This particle can be identified from  $B \rightarrow K\bar{K}K$  and  $B \rightarrow K\eta\pi$  decays. Knowing this decay rate the other parameters in the model for the given decay multiplets can be determined more directly. Alternatively,  $a_0(1450)$  could be the nonet partner of  $f_0(980)$ .

The  $a_0(980)$  rate would help in particular in a judgement about the classification with  $f_0(980)$  as heaviest particle in the nonet together with  $\sigma$  and  $\kappa$  in  $B$  decays. At present there is no strong indication for the presence of these particles but a more dedicated analysis in the determination of the respective decay rates is necessary.

The study of charmless  $B$  decays into the various members of the nonet represents a systematic approach to scalar spectroscopy which can be followed in great analogy to the successful phenomenology of the decays into pseudoscalars. A particularly interesting test is the comparison of decays  $PS$  and  $VS$  with  $K$  and  $K^*$  which are expected in some cases with quite different rates because of different signs of the parameter  $\beta$ . Our first attempts indicate a different sign of the amplitudes  $\gamma, \beta$  in final states with scalar and pseudoscalar particles.

Finally, we come back to the question of gluonic meson production. First there is the gluonic component in the production of isoscalar mesons which is obtained for  $\eta, \eta'$  already in previous analyses. We find such components also in the scalar sector for  $f_0(980)$ . A more definitive analysis can be done given the  $a_0$  rates.

The presence of a coherent background can be derived from its interference with  $f_0(1500)$ . In our glueball interpretation we expect a production phase moving slowly with energy according to a Breit–Wigner amplitude with some modification by inelastic effects. It will be interesting to determine more accurately the interference between the background (gb) and  $f_0(980)$  whether it is destructive (as in  $J/\psi \rightarrow \phi\pi\pi$  and in our model) or constructive; this has a big influence on the derivation of the important  $f_0(980)$  decay rate. The  $\pi\pi/K\bar{K}$  branching ratios of the background from our estimate are consistent with this glueball hypothesis. Furthermore we predict a sizable  $\eta\eta$  and, at higher masses, a  $4\pi$  decay rate.

The broad background has also shown up in other gluonic processes like double pomeron production and  $p\bar{p}$  annihilation, also with a suppressed rate in  $\gamma\gamma$  collisions [75,76]; on the other hand, it has been difficult to see its sign in  $J/\psi \rightarrow \pi\pi\gamma$ ,  $K\bar{K}\gamma$  (see discussion in [32]). Recent high statistics results by BES [77] on  $K\bar{K}\gamma$ , however, require a broad  $0^{++}$  coherent background for a good description of the data as well. We have no definitive explanation why  $\mathcal{B}(J/\psi \rightarrow f_0(980)\gamma)$  is apparently much smaller than  $\mathcal{B}(J/\psi \rightarrow \eta'\gamma)$  despite the similar quark structure proposed for  $f_0(980)$  and  $\eta'$ . A possible explanation is a destructive interference with the background, seen in other processes as discussed, such that the appearance of  $f_0(980)$  is minimized, but also a special effect in the exclusive decay could be thought of. Therefore, it would be interesting to see whether the similarity of  $\eta'$  and  $f_0(980)$  is recovered in the fragmentation region of gluon jets as discussed in [8].

It remains an interesting question how the  $b \rightarrow sg$  decay is realized by hadronic final states. The large rate for the  $0^{++}$  glueball we obtain within our approach suggests the intriguing possibility that it could be saturated by gluonic mesons. In the next step it will be interesting to search for the  $0^{-+}$  glueball which could decay into  $\eta\pi\pi$  and  $K\bar{K}\pi$ .

## References

1. A. Garmash et al. (BELLE Collaboration), Phys. Rev. D **65**, 092005 (2002)
2. K. Abe et al., Study of charmless  $B$  decays to three-Kaon final states, BELLE-CONF-0225, hep-ex/0208030

3. K. Abe et al., Study of the three-body charmless  $B^+ \rightarrow K^+\pi^+\pi^-$  and  $B^+ \rightarrow K^+K^+K^-$  decays, BELLE-CONF-0338, EPS Conference contribution EPS-ID 577 (2003); <http://belle.kek.jp/conferences/LP03-EPS/>
4. A. Garmash et al. (BELLE Collaboration), Phys. Rev. D **69**, 012001 (2004)
5. B. Aubert et al. (BaBar Collaboration), Measurements of the Branching Fractions of Charged  $B$  Decays to  $K^+\pi^-\pi^-$  Final states, hep-ex/0308065v2
6. B. Aubert et al., Measurements of the Branching Fractions of charmless three-body charged  $B$  Decays, BaBar-Conf-02/009, hep-ex/0206004
7. P. Minkowski, W. Ochs, Scalar meson and glueball in  $B$  decays and gluon jets, hep-ph/0304144
8. P. Minkowski, W. Ochs, Gluonic meson production, in Proceedings of the Ringberg workshop New Trends in HERA physics 2003, September 2003, edited by G. Grindhammer et al., (World Scientific, Singapore 2004), p.169; hep-ph/0401167; Phys. Lett. B **485**, 139 (2000)
9. V. Chernyak, Phys. Lett. B **509**, 273 (2001)
10. B.H. Behrens et al., Phys. Rev. Lett. **80**, 3710 (1998)
11. T.E. Browder et al., Phys. Rev. Lett. **81**, 1786 (1998)
12. S.J. Richichi et al. Phys. Rev. Lett. **85**, 520 (2000)
13. K. Abe et al., Phys. Lett. B **517**, 309 (2001)
14. B. Aubert et al., Phys. Rev. Lett. **87**, 221802 (2001)
15. D. Atwood, A. Soni, Phys. Rev. Lett. **79**, 5206 (1997)
16. H. Fritzsche, Phys. Lett. B **415**, 83 (1997)
17. X.-G. He, W.-S. Hou, C.-S. Huang, Phys. Lett. B **429**, 99 (1998)
18. A.S. Dighe, M. Gronau, J.L. Rosner, Phys. Lett. B **367**, 357 (1996); Phys. Rev. Lett. **79**, 4333 (1997)
19. M. Ciuchini, E. Franco, G. Martinelli, L. Reina, L. Silvestrini, Phys. Lett. B **334**, 137 (1994)
20. C. Greub, P. Liniger, Phys. Rev. D **63**, 054025 (2001)
21. G. Altarelli, S. Petrarca, Phys. Lett. B **261**, 303 (1991)
22. A. Lenz, U. Nierste, G. Ostermaier, Phys. Rev. D **56**, 7228 (1997)
23. P. Minkowski, Phys. Lett. B **88**, 938 (1979)
24. K. Hagiwara et al. (Particle Data Group), Phys. Rev. D **66**, 010001 (2002); <http://pdg.lbl.gov>
25. G. Bali et al., Phys. Lett. B **309**, 378 (1993)
26. J. Sexton, A. Vaccarino, D. Weingarten, Phys. Rev. Lett. **75**, 4563 (1995)
27. C.J. Morningstar, M. Peardon, Phys. Rev. D **60**, 034509 (1999)
28. B. Lucini, M. Teper, JHEP **0106**, 050 (2001)
29. G.S. Bali, in Fourth International Conference on Perspectives in Hadronic Physics, ICTP, Trieste, Italy, May 2003; hep-lat/0308015
30. A. Hart, M. Teper, Phys. Rev. D **65**, 034502 (2002)
31. A. Hart, C. McNeile, C. Michael, Nucl. Phys. B (Proc. Suppl.) **119**, 266 (2003)
32. P. Minkowski, W. Ochs, Eur. Phys. J. C **9**, 283 (1999)
33. B. Hyams et al., Nucl. Phys. B **64**, 134 (1973); W. Ochs, Ludwig-Maximilians-University Munich, thesis 1973 (unpublished)
34. D. Morgan, M.R. Pennington, Phys. Rev. D **48**, 1185 (1993)
35. P. Minkowski, W. Ochs, Nucl. Phys. B (Proc. Suppl.) **121**, 119 (2003); hep-ex/0209223
36. P. Minkowski, W. Ochs, Nucl. Phys. B (Proc. Suppl.) **121**, 123 (2003); hep-ex/0209225
37. E. Klempt, B.C. Metsch, C.R. Münz, H.R. Petry, Phys. Lett. B **361**, 160 (1995)
38. E. Klempt, Meson Spectroscopy: Glueballs, Hybrids and  $Q\bar{Q}$  Mesons, PSI Zuoz Summer School, August 2000, hep-ex/0101031
39. S. Narison, Nucl. Phys. B **509**, 312 (1998); A **675**, 54c (2000)
40. E. Bagan, T.G. Steele, Phys. Lett. B **243**, 413 (1990); T.G. Steele, D. Harnett, G. Orlandini, hep-ph/0308074
41. H. Forkel, hep-ph/0312049
42. V.V. Anisovich, Yu.D. Prokoshkin, A.V. Sarantsev, Phys. Lett. B **389**, 388 (1996); V.V. Anisovich, A.V. Sarantsev, Eur. Phys. J. A **16**, 229 (2003)
43. C. Amsler, F.E. Close, Phys. Lett. B **353**, 385 (1995); Phys. Rev. D **53**, 295 (1996); F.E. Close, A. Kirk, Phys. Lett. B **483**, 345 (2000)
44. W. Lee, D. Weingarten, Phys. Rev. D **61**, 014015 (2000)
45. D. Morgan, Phys. Lett. B **51**, 71 (1974)
46. M. Roos, N.A. Törnqvist, Phys. Rev. Lett. **76**, 1575 (1996)
47. M.D. Scadron, G. Rupp, F. Kleefeld, E. van Beveren, Phys. Rev. D **69**, 014010 (2004); Erratum D **69**, 059901 (2004)
48. S. Ishida, M. Ishida, Phys. Lett. B **539**, 249 (2002)
49. R.L. Jaffe, Phys. Rev. D **15**, 267, 281 (1977)
50. N.N. Achasov, S.A. Devyanin, G.N. Shestakov, Z. Phys. C **22**, 53 (1984); N.N. Achasov, V.V. Gubin, Phys. Rev. D **63**, 094007 (2001)
51. D. Black, A.H. Fariborz, F. Sannino, J. Schechter, Phys. Rev. D **59**, 074026 (1999)
52. J.A. Oller, E. Oset, J.R. Pelaez, Phys. Rev. D **59**, 074001 (1999)
53. F.E. Close, N.A. Törnqvist, Phys. G28 (2002) R249
54. S.F. Tuan, in Hadron Spectroscopy, Chiral Symmetry and Relativistic Description of Bound Systems, Tokyo, Japan, February 2003, edited by S. Ishida et al., KEK Proc. 2003-7; hep-ph/0303248
55. C. Amsler, N.A. Törnqvist, Phys. Rep. **389**, 61 (2004)
56. S. Cherry, M.R. Pennington, Nucl. Phys. A **688**, 823 (2001)
57. W. Ochs, The scalar meson sector and the  $\sigma$ ,  $\kappa$  problem, in HADRON'03, Aschaffenburg, Germany, August 2003, to appear in AIP Conf. Proc., hep-ph/0311144
58. G. Colangelo, J. Gasser, H. Leutwyler, Nucl. Phys. B **603**, 125 (2001)
59. U.G. Meissner, Comm. Nucl. Part. Phys. **20**, 119 (1991)
60. A. Ali, G. Kramer, C.-D. Lu, Phys. Rev. D **58**, 094009 (1998)
61. A. Ali, C. Greub, Phys. Rev. D **57**, 2996 (1998)
62. A. Ali, J. Chay, C. Greub, P. Ko, Phys. Lett. B **424**, 161 (1998)
63. M. Beneke, M. Neubert, Nucl. Phys. B **651**, 225 (2003); B **675**, 333 (2003)
64. C.W. Chiang, J.L. Rosner, Phys. Rev. D **65**, 074035 (2002); M. Gronau, J.L. Rosner, Phys. Rev. D **61**, 073008 (2000)
65. H. Fritzsche, P. Minkowski, Nuov. Cim. A **30**, 393 (1975); P. Minkowski, Central hadron production in crossing of dedicated hadronic beams, hep-ph/0405032
66. C.W. Chiang, M. Gronau, Z. Luo, J.L. Rosner, D.A. Suprun, Phys. Rev. D **69**, 0340 (2004)
67. H.J. Lipkin, Phys. Lett. B **415**, 186 (1997)
68. M. Bargiotti et al., Eur. Phys. J. C **26**, 371 (2003)
69. A. Abele et al., Phys. Rev. D **57**, 3860 (1998)
70. E.M. Aitala et al. (E791 Collaboration), Phys. Rev. Lett. **89**, 121801 (2002)
71. D. Barberis et al. (Omega Collaboration), Phys. Lett. B **462**, 462 (1999)

72. A. Falvard et al. (DM2 Collaboration), Phys. Rev. D **38**, 2706 (1988)
73. J. Reinnarth, Ph.D. thesis, University Bonn, 2003
74. E. Klempt, Glueballs, Hybrids, Pentaquarks, 18th Annual Hampton University Graduate Studies Jefferson Lab, Newport News, Virginia, June 2003, hep-ex/0404270
75. M. Boglione, M.R. Pennington, Eur. Phys. J. C **9**, 11 (1999)
76. P. Minkowski, W. Ochs, Workshop on Hadron Spectroscopy, edited by T. Bressani, A. Feliciello, A. Filippi, Frascati Physics Series **15**, 245 (1999)
77. J.Z. Bai et al. (BES Collaboration), Phys. Rev D **68**, 052003 (2003)